Journal of Power Sources 206 (2012) 476–482

Contents lists available at SciVerse ScienceDirect

Journal of Power Sources

journal homepage: www.elsevier.com/locate/jpowsour

Graphene based supercapacitor fabricated by vacuum filtration deposition

Sanliang Zhang[a], Yueming Li[b], Ning Pan[a,b,*]

[a] Department of Biological and Agricultural Engineering, University of California at Davis, CA 95616, United States
[b] Nanomaterials in the Environment, Agriculture, and Technology (NEAT), University of California at Davis, CA 95616, United States

ARTICLE INFO

Article history:
Received 14 October 2011
Received in revised form 19 January 2012
Accepted 21 January 2012
Available online 28 January 2012

Keywords:
Electrophoretic deposition
Graphene nanosheets
Supercapacitor
Vacuum filtration deposition

ABSTRACT

A novel method involving vacuum filtration deposition (VFD) of graphene suspension is developed in this study to fabricate graphene based nickel foam electrode for supercapacitor. Acid-treated graphene nanosheets in a suspension can be easily deposited in the pores of nickel foam in large quantity using this method, *thus producing supercapacitors with large energy capacity*. Structural and morphological characterizations of as prepared electrodes have been carried out using scan electron microscopy (SEM), energy-dispersive X-ray spectroscopy (EDS), Fourier transform infrared spectroscopy (FTIR), and Raman spectroscopy. Electrochemical performance of as prepared electrode has also been investigated through cyclic voltammetry, electrochemical impedance spectroscopy, and galvanostatic charge/discharge analyzer, in comparison with electrodes prepared via existing technique. Our results demonstrated that the new electrode, while achieving much greater energy capacity due to large active substance incorporated, still maintains a relatively high power density and a good cycle performance in 6 M KOH electrolyte. Our results also demonstrated that a supercapacitor made of the existing electrophoretic deposition based electrodes will lose its entire capacitance after certain time period (20 days in our study); whereas the VFD based one retains virtually all its performance after the same period. The present study shows the potential application of this method for fabrication of supercapacitor with much improved energy capacity.

1. Introduction

Supercapacitor, also called ultracapacitor or electrochemical capacitor, has been intensively studied in recent years owing to its unique property [1–3]. It differs from the conventional dielectric capacitors in its special energy storage modes, including Faradic process and capacitive process [4–6], leading to its significantly improved energy density (usage life after one charge) and power density (rate of discharge). If the energy capacity can be further increased, it can be used in much wider array of fields such as hybrid electric vehicle [2], fuel cell/battery/supercapacitor hybridization [7], backup or alternation power source, engine starting system, electric actuator, and telecommunication [3].

Of the existing electrode fabrication techniques for supercapacitors, the drop-drying method [6,8,9], spray deposition [10,11], and Meyer rod coating [12] deploy the working materials loosely onto the metal current collector, resulting in electrodes with very high internal resistance due to poor contact in the working media and between the working media and the metal current collector. The other techniques including electrophoretic deposition (EPD) [4,13], electrostatic spray deposition (ESD) [14], electrodeposition [15], and layer-by-layer assembly [16], while improving the internal binding and thus producing electrodes with very small resistant and excellent response, can only incorporate limited active materials into the electrodes [17]. As a result, the supercapacitors thus prepared *cannot* store sufficient electricity for most practical applications.

There are a couple issues to clarify when dealing with supercapacitor performance. Of the two main parameters used, i.e., energy density (usage life after one charge) and power density (rate of discharge), the power density or the rate of response for supercapacitor is already sufficient for most applications, it is the usage life or the energy stored, that is the main drawback for supercapacitors when being considered for more power demanding usages. In addition, there are many reported supercapacitors developed from laboratory showing high values in both *specific* energy and power densities. But, they only look attractive in terms of per unit weight, not in actual or absolute power.

Our challenge therefore was to develop an electrode fabrication technique which not only makes electrodes with satisfactory electrochemical response, but also incorporates into the electrodes sufficiently large amount of active substance for power storage. Naturally, this new technique should have the potential to scale up for industrial manufacturing.

* Corresponding author at: Nanomaterials in the Environment, Agriculture, and Technology (NEAT), University of California at Davis, CA 95616, United States. Tel.: +1 530 752 6232; fax: +1 530 752 7584.
E-mail address: npan@ucdavis.edu (N. Pan).

0378-7753/$ – see front matter © 2012 Elsevier B.V. All rights reserved.
doi:10.1016/j.jpowsour.2012.01.124

Researches [13,17] have already tried to increase the amount of active materials deposited by using substrates with larger specific surface area, like metal foams. As to the working media, graphene has attracted huge interest owing to some novel properties [18]. Graphene presents remarkable mechanical property, good chemical and thermal stability, excellent electronic conductivity, and large surface area [19–21], making it a suitable candidate for electrochemical energy storage devices, such as in Li-ion battery [22–24], hydrogen fuel cells [25,26], and supercapacitor [5,27,28].

We have developed a simple electrode fabrication method, not seen reported before, in this study in which a vacuum filtration was used to disperse the graphene nanosheets in solution into the pores of nickel foam to form electrodes. Although this method may appear similar to the ordinary filtration method which has been utilized to fabricate electrodes, for instance, by Du and Pan [29], Bispo-Fonseca et al. [30], and Cooper et al. [31], there are several significant differences between them. The ordinary filtration method involves multiple steps, yields electrodes with significantly larger internal contact resistance and thus poor electrochemical performance, and is only able to incorporate small amount of working media into the electrodes.

Electrochemical experiments showed that the new electrodes from this study retained high power density (38 kW kg^{-1}). Unlike EPD method, however, the quantity of the active materials in the electrode, thus the energy capacity of the supercapacitor, can be facilely adjusted over a large range using our new method. Furthermore, the as-prepared electrodes achieved good retention ratio of original capacitance after 20 days, while the EPD cells lost virtually all the energy stored. In general, our testing results demonstrated that this vacuum filtration method, readily expandable to industrial scale, may be a very promising approach for supercapacitor electrode fabrication.

2. Experimental

2.1. Materials and methods

In this study, we first prepared graphene based supercapacitors using the new vacuum filtration deposition (VFD) method. Graphene nanoplatelets (grade M) were purchased from XG sciences. As-received graphene nanoplatelets were refluxed with boiling concentrated nitric acid (68%) for 10 h, and then thoroughly washed with distilled water followed by drying at 100 °C in vacuum. The refluxed graphene as active material, and poly(vinylidene fluoride) (PVDF) powder (4:1 wt.%) as both the binder to the current collector and the contributor to the mesopores formation, were mixed and dissolved in absolute ethanol, and then stirred in 50 °C water bath for 2 h followed by 90 min intensive ultrasonication to form a homogenous mixture. The mixture was then forced to penetrate into the nickel foam through vacuum filtration deposition process as illustrated in Fig. 1, and the finished nickel foam to make the current collector was then dried at 100 °C in vacuum. The nickel foam was purchased from MarkTech International, Inc., with the thickness of 2.0 ± 0.1 mm, porosity of 95%, and pore size of 100 ppi. Therefore, the total pore volume of an 1.2 cm diameter foam is:

$$V_{\text{pore}} = \frac{\pi}{4} \times 1.2^2\,\text{cm}^2 \times 0.2\,\text{cm} \times 95\% \approx 0.215\,\text{m}^3$$

It is clear from the illustration that by adjusting the vacuum pressure and process duration, we can control the amount and the distribution of the working media into the porous metal foam. In fact, that amount is only limited by the concentration in the mixture, and the porosity of the foam. The working media filtrated into the pores bound with the foam much closely than deposited merely on its surface. Finally, scaling up the set-up in the figure presents no major difficulty.

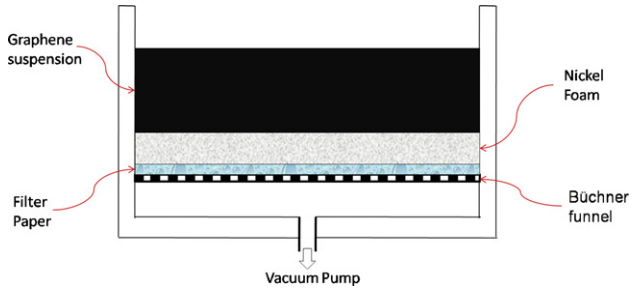

Fig. 1. Schematic of vacuum filtration deposition process (VFD).

Meanwhile for comparison, electrophoretic deposition (EPD) method was also used to prepare the electrodes. As proposed previously by our group [29], 10^{-5}–10^{-4} mol of $Mg(NO_3)_2$ as the charger was added into a mixture of graphene and polyacrylic acid (PAA), and the mixture was then subjected to 50 V DC voltage with two pieces of nickel foam as the anode and cathode. After 13 min, graphene were deposited onto the cathode nickel foam.

Then, four electrodes of 12 mm diameter, two from each method, were molded from the prepared nickel foams by a precision disc cutter, and followed by a rolling press to 0.4 and 0.2 cm thickness for VFD and EPD prepared electrodes respectively. The as-made electrodes were then heat-treated at 900 °C for 30 min in argon gas. After that, two pairs of electrodes from each method were constructed into a supercapacitor by using a glass microfiber filter paper as the separator soaked with 6 M KOH electrolyte. Two coin supercapacitors were thus prepared using MT-180 manual crimping machine with dies for CR2032 coin cell.

2.2. Characterization

The surface morphologies of the pristine graphene powder and as-deposited electrode were inspected by Scan Electron Microscopy. Energy-dispersive X-ray spectroscopy (EDS), Fourier transform infrared spectroscopy (FT-IR) and Raman spectroscopy were used to investigate the chemical properties of the graphene materials at different stages throughout the process.

The electrochemical properties of the supercapacitors were analyzed through cyclic voltammetry (CV) on a potentiostat/galvanostat (EG&G Princeton Applied Research, Model 263A), galvanostatic charge/discharge on an eight channels battery analyzer (MTI Corporation, mode BST8-MA), and electrochemical impedance spectroscopy (EIS) on a frequency response detector connected with the EG&G 263A with the frequency from 100 kHz to 10 MHz at room temperature.

3. Result and discussion

Our VFD fabrication method was inspired by the VARTM (vacuum assistant resin transfer molding) used in composite manufacturing industry, and illustrated in Fig. 1. As we mentioned, the graphene nanosheets could thus be massively deposited into the pores of nickel foam. The surface morphologies of the pristine graphene powder and as-deposited electrode were inspected by field-emission scan electron microscopy. Fourier transform infrared spectroscopy (FT-IR) and Raman spectroscopy were used to investigate the chemical properties of the graphene materials at different stages throughout the process. Fig. 2a shows the morphology of the pristine graphene powder comprised of graphene platelets with the average diameters of approximately 5–10 μm and average thickness of 6–8 nm. SEM image in Fig. 2b demonstrated the overall structure of the as-prepared acid-treated graphene electrode, and Fig. 2c shows that the morphology of

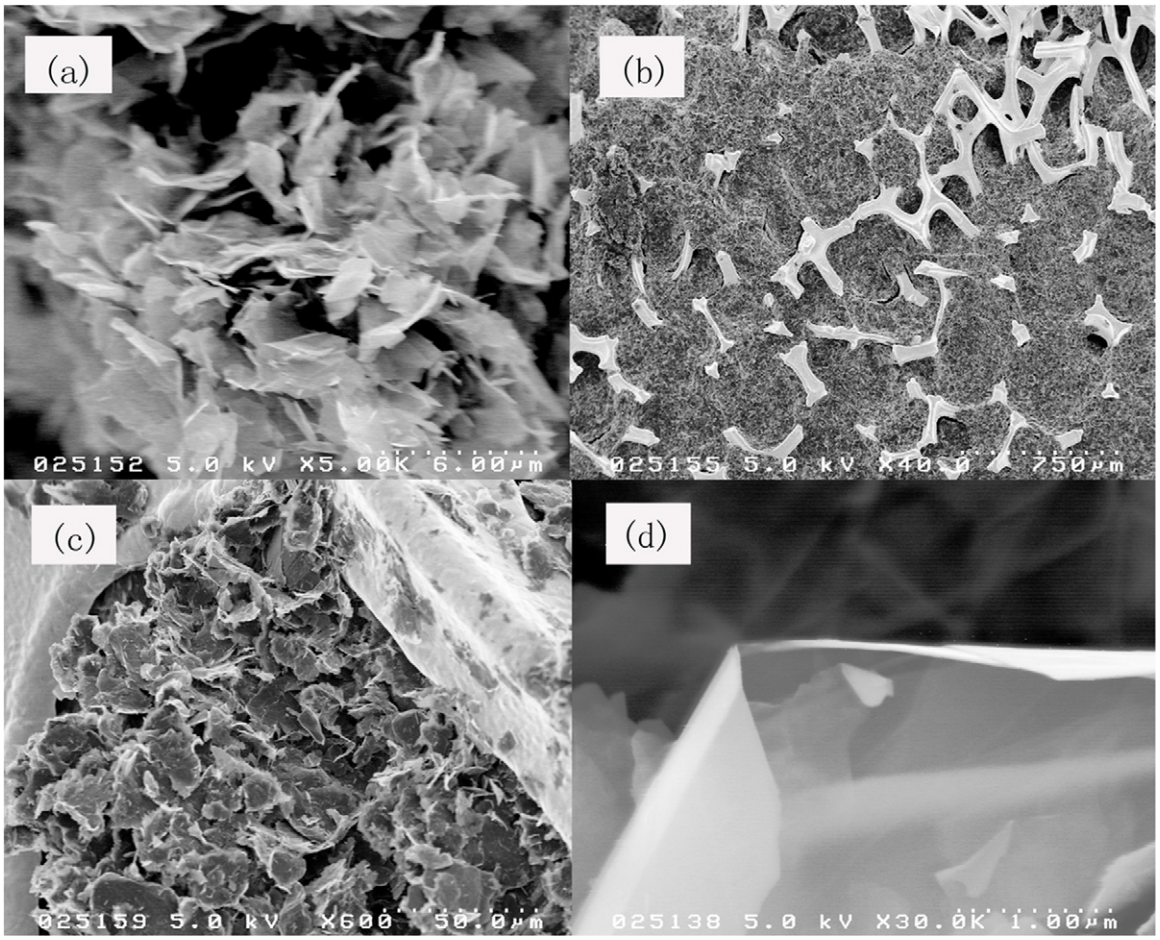

Fig. 2. SEM images of pristine graphene powder (a), low (b), middle (c), and high (d) magnifications of as-deposited graphene electrode.

the graphene materials in the pores of nickel foam. The graphene platelet in Fig. 2d retained its 2D structure without major changes from the pristine state, and this planar structure was considered to rise to the edge effects and large accessible surface area for charge accumulation [19–21].

The functional groups in the pristine graphene, acid-treated graphene, and heat-treated graphene were studied by Fourier transform infrared spectroscopy recorded on a Nicolet 6700 spectrometer. The spectra confirmed the presence of hydroxyl O—H (ν_{O-H} at 3452 cm^{-1} and 3435 cm^{-1}), C—OH (ν_{C-O} at 1384 cm^{-1}), alkane C—H (ν_{C-H} at 2920 cm^{-1}), and aromatic C=C ($\nu_{C=C}$ at 1631 cm^{-1}) [32]. From the comparison of FTIR spectra of pristine graphene (PG) and acid-treated graphene (AG) in Fig. 3a, the peak at 1105 cm^{-1}, identified as stretching vibration of C—O [32,33] functional group, was effectively intensified after acid treatment. This intensification greatly increased the solubility of graphene in ethanol. However, the peak at 1384 cm^{-1} for heat-treated graphene (HG) was severely attenuated, implying a substantial elimination of hydroxyl functions.

The spectra of energy dispersive X-ray spectroscopy (EDS) in Fig. 4 indicated the elemental composition of as-made graphene based electrode. Obviously, the three patterns were almost identical, with only a small difference in the atomic composition. According to the quantitative analysis of EDS, the atomic ratios of carbon to oxygen were 22, 21, and 27, correspondingly to PG, AG and HG. The results indicated that the oxygen content slightly increased after acid treatment and considerable amount of oxygen containing groups were eliminated by heat treatment, which were consistent with the FT-IR spectra in Fig. 3a.

The Raman spectra in Fig. 3b showed the structural differences among pristine graphene (PG), acid-treated graphene (AG), and heat-treated graphene (HG). The D-bands near 1355 cm^{-1} as defects induced bands are due to the A_{1g} mode breathing vibration in the hexagonal sp^2 carbon rings when adjacent carbon is converted into sp^3 hybridized graphitic material. The G-bands near 1580 cm^{-1}, and 2D-bands near 2724 cm^{-1} are two characteristic peaks of graphene material, owing to the E_{2g} vibration mode of the hexagonal sp^2 carbon rings and phonons scattering at zone boundary, respectively [34–38]. Meanwhile the I_D/I_G ratio decreased from 0.311 for PG to 0.176 for AG, indicating the enhancement of purity of graphene material [36,39]. The attenuation of D-band for HG furnished a very small I_D/I_G ratio 0.075, known as a symbol of graphene materials [34]. Overall, the active material in our electrodes was characterized as relatively pure graphene material.

Cyclic voltammetric (CV) curves for both EPD and VFD prepared graphene electrodes are shown in Fig. 5 under different scan rates from 10 $mV\,s^{-1}$ to 50 $mV\,s^{-1}$. Although both cases yielded very small internal resistant as reflected by the sharp charge and discharge processes, the VFD results exhibited fairly rectangular CV curves, at all scan rates from 10 to 50 $mV\,s^{-1}$. From another perspective, the almost ideal rectangular CV curves from VFD electrodes reflect small contact resistance due to close connection between the graphene nanosheets and the nickel foam. More importantly, the VFD electrodes generated electric current one order of magnitude greater than that by EPD electrodes. This indicated that the total energy capacity of the VFD electrode based supercapacitor is much greater, owing to the large quantity

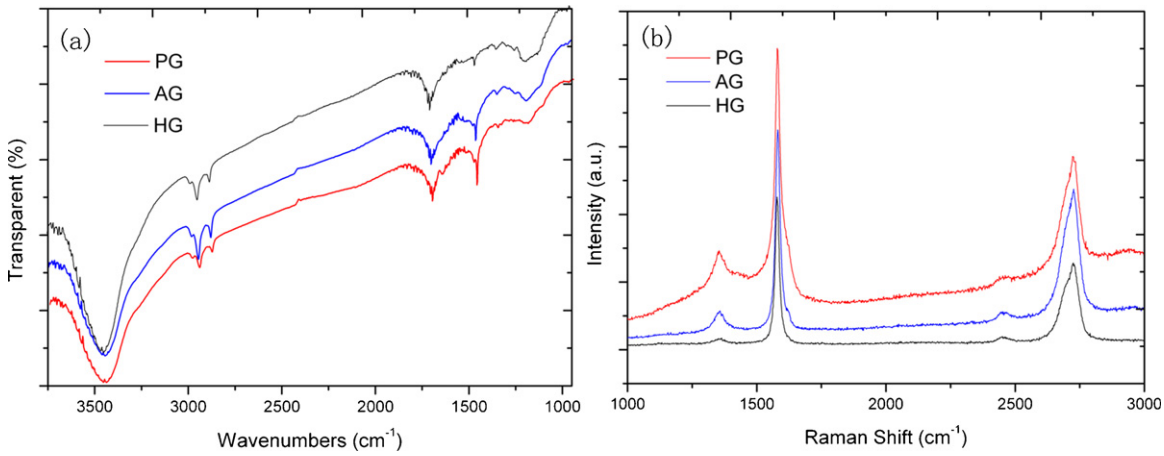

Fig. 3. FT-IR and Raman spectra of pristine graphene (PG) with red line, acid-treated graphene (AG) blue line, and heat-treated graphene (HG) black line. (For interpretation of the references to color in this figure legend, the reader is referred to the web version of this article.)

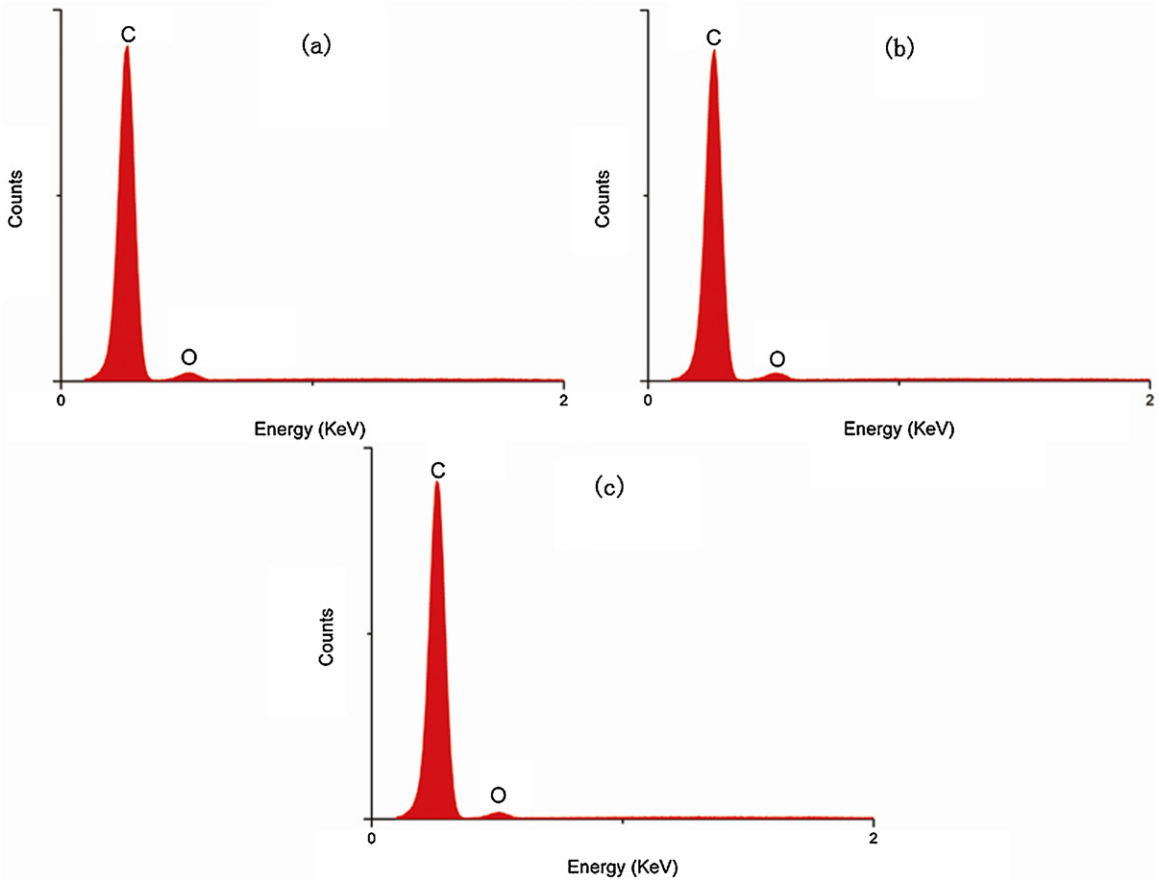

Fig. 4. EDS spectra of pristine graphene (a), acid-treated graphene (b), and heat-treated graphene (c).

of deposited graphene in its current collector, whereas the EPD method is only able to incorporate very tiny amount of working media into the electrodes, as compared in Table 1.

In addition, at a given scan rate, e.g., 10 mV s^{-1}, the *specific* capacitance of electrodes derived from the CV curves was 120 F g^{-1} for EPD electrode, smaller than 152 F g^{-1} for VFD one. In fact, in all the *specific* terms such as specific capacitance and energy density, the two techniques led to comparable results. It is in the absolute or actual capacitance, VFD is far superior to its EPD counterparts. Actually, to examine the application potential, it makes much more sense to compare in such absolute terms.

Table 1
Relationship between deposited graphene mass and cell capacitance under 10 mV s^{-1}.

Electrode	Deposited grapheme (mg)	Calculated cell capacitance (F)
EPD	0.8	0.024
VFD1	3.4	0.150
VFD2	12.0	0.470
VFD3	17.8	0.702

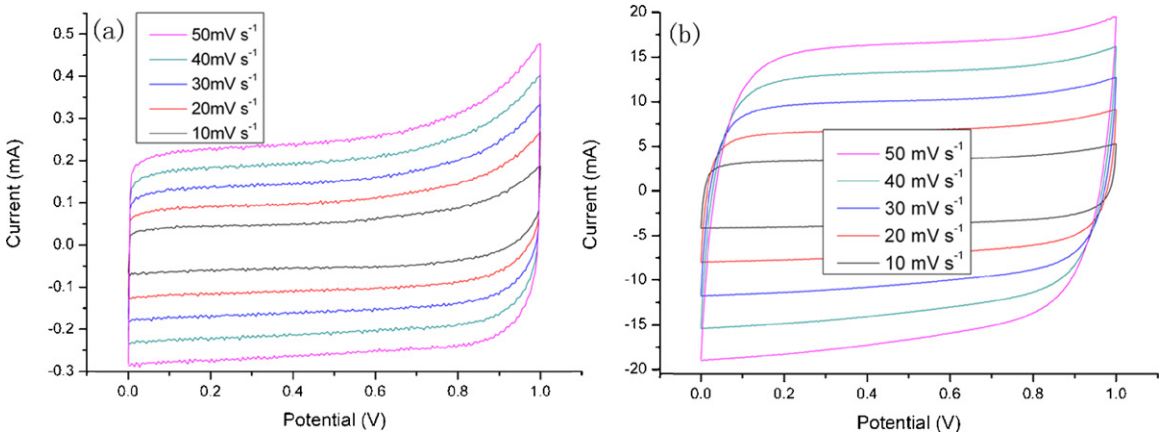

Fig. 5. The cyclic voltammetric (CV) curves of EPD prepared (a), and VFD prepared (b) graphene electrodes under different scan rates.

To further demonstrate the advantages of the VFD technique, Table 1 shows that using VFD we can readily increase the graphene mass deposited in the 1.2 cm diameter nickel foam so as to adjust the overall cell capacitance, as compared with the fixed low values achieved by the EPD method.

Still, the maximum *specific* capacitance we achieved currently using VFD is 152 F g^{-1} based on the corresponding mass of single electrode under the scan rate of 10 mV s^{-1}. Although this specific capacitance is no greater than some of the values reported by other researchers using graphene as electrode materials, we can always increase this number by using the graphene material chemically reduced from graphene oxide [5,40]. In other words, increasing the specific values is not the focus of this study.

Also, the freshly made test cells demonstrated excellent cycling repeatability within the first 2000 cycles for the electrodes prepared by both methods. In fact, both methods furnished a high retention ratio of >95% for the first 2000 cycles.

We then compared the performance retention ability over time between the two methods. Fig. 6 shows respectively the CV curves for EPD and VFD electrodes at 10 mV s^{-1}, tested 20 days apart. However, after 20 days the capacitance in the EPD electrodes decreased so dramatically that its CV curve reduced into a straight line, while the VFD cell showed virtually no loss as seen in the Fig. 6. This indicates that the stability of VFD prepared electrode is much better than the EPD one. To the best of our knowledge, there has no published result about this phenomenon, and in our opinion, this deterioration was probably attributable to the formation of sp^3 hybridized carbons in the active substance due to certain redox reaction or detachment of graphene material from the nickel surface. It is speculated that the graphene materials were much more deeply penetrated into the internal pores of the nickel foam under the high vacuum pressure during the VFD process, thus furbishing a much secure binding between them, than in the case of EPD where contact between the working media and the nickel foam is more superficial.

From the complex-plane impedance plots in Fig. 7, the values at *X*-axis, the corresponding real impedance, reflected a very small equivalent series resistant (ESR) for the supercapacitors from both methods. The ESR was 274 mΩ for VFD electrodes, slightly larger than 219 mΩ for EPD samples, confirming the results in Fig. 8. The charge–discharge curves of EPD and VFD cells in Fig. 8 revealed the corresponding IR drops of 16 mV and 21.1 mV, respectively. The smaller ESR would give rise to larger power density P_{max} according to the equation of $P_{max} = V^2/4MR$ [41] (where V is the initial voltage, R is the ESR of the test cell, and M the combined graphene mass of two electrodes). Using the ESR = 274 mΩ for VFD electrodes, the calculated power density was about 38 kW kg^{-1}. The power density of the electrode calculated through the integration of the inner integrated area of the CV curve [42], a common practice, was not used, because the value varies directly to the scan rate and the potential window.

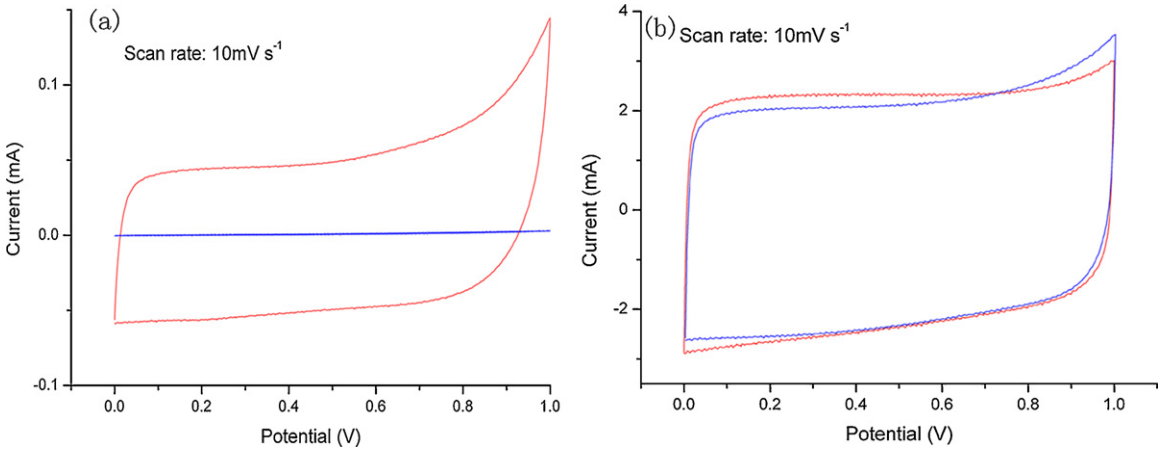

Fig. 6. The cyclic voltammetric (CV) curves of as-made (red line) and 20 days old (blue line) electrodes prepared by EPD (a) and VFD (b). (For interpretation of the references to color in this figure legend, the reader is referred to the web version of this article.)

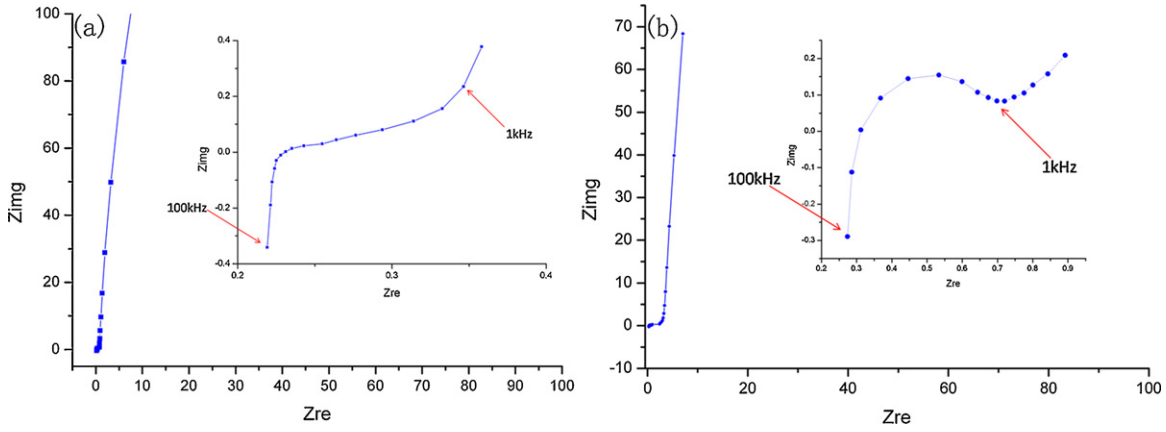

Fig. 7. Complex-plane impedance plots (Nyquist plots) of the graphene electrodes prepared by EPD method (a) and VFD method (b) from 100 kHz to 10 MHz. Zimg: imaginary impedance, Zre: real impedance, they both share the units of ohms.

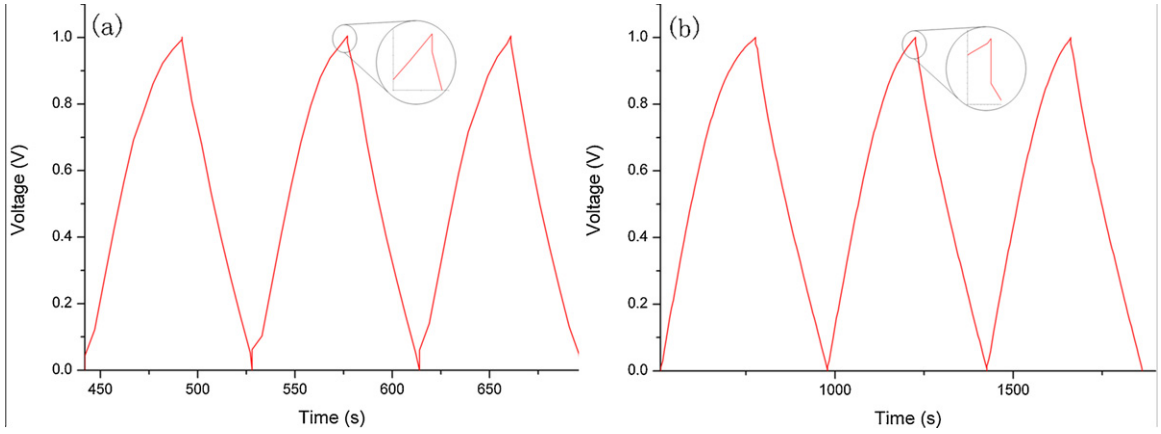

Fig. 8. Charge–discharge curves of as-made grahpene electrodes through EPD (a), and VFD (b) method under current density of 1 mA cm^{-2}.

4. Conclusion

In this paper, we developed a novel way for electrode fabrication, the vacuum filtration deposition (VFD) method, employing vacuum pressure to penetrate graphene materials in solution into the pores of nickel foam to form the electrodes for supercapacitor. The process is simple, easy to scale up and more importantly, able to incorporate large amount of working media into an electrode thus to yield supercapacitors with much larger energy capacities, overcoming the bottleneck problem associated with existing techniques. From our preliminary experiment results, the as-fabricated electrode also maintained high *power* density as well as good cycle performance.

Our results also demonstrated that a supercapacitor made of EPD based electrodes will lose its entire capacitance after certain time period (20 days in our study); whereas the VFD based one retains virtually all its performance after the same period, another significant advantage of the VFD process. In summary, we consider the VFD process a highly promising method which can produce supercapacitors with exceptionally high energy capacity and superior stability.

Acknowledgement

The authors acknowledge the partial financial support provided by the California Energy Commission under the Grant number 55697A/07-21.

References

[1] Y. Zhu, S. Murali, M.D. Stoller, K.J. Ganesh, W. Cai, P.J. Ferreira, A. Pirkle, R.M. Wallace, K.A. Cychosz, M. Thommes, D. Su, E.A. Stach, R.S. Ruoff, Science 332 (2011) 1537.
[2] A. Burke, J. Power Sources 91 (2000) 37.
[3] R. kötz, M. Carlen, Electrochim. Acta 45 (2000) 2483.
[4] C. Du, N. Pan, Nanotechnology 17 (2006) 5314.
[5] M.D. Stoller, S. Park, Y. Zhu, J. An, R.S. Ruoff, Nano Lett. 8 (2008) 3498.
[6] K.H. An, W.S. Kim, Y.S. Park, J.-M. Moon, D.J. Bae, S.C. Lim, Y.S. Lee, Y.H. Lee, Adv. Funct. Mater. 11 (2001) 387.
[7] P. Thounthong, S. Raël, B. Davat, J. Power Sources 193 (2009) 376.
[8] A. Izadi-Najafabadi, T. Yamada, D.N. Futaba, M. Yudasaka, H. Takagi, H. Hatori, S. Iijima, K. Hata, ACS Nano 5 (2011) 811.
[9] C.-Y. Liu, A.J. Bard, F. Wudl, I. Weitz, J.R. Heath, Electrochem. Solid-State Lett. 2 (1999) 577.
[10] X. Zhao, B.T.T. Chu, B. Ballesteros, W. Wang, C. Johnston, J.M. Sykes, P.S. Grant, Nanotechnology 20 (2009) 065605.
[11] M. Kaempgen, C.K. Chan, J. Ma, Y. Cui, G. Gruner, Nano Lett. 9 (2009) 1872.
[12] L. Hu, J.W. Choi, Y. Yang, S. Jeong, F. La Mantia, L.F. Cui, Y. Cui, Proc. Natl. Acad. Sci. U.S.A. 106 (2009) 21490.
[13] Y. Chen, X. Zhang, P. Yu, Y. Ma, J. Power Sources 195 (2010) 3031.
[14] J. Kim, K. Nam, S. Ma, K. Kim, Carbon 44 (2006) 1963.
[15] H. Li, J. Wang, Q. Chu, Z. Wang, F. Zhang, S. Wang, J. Power Sources 190 (2009) 578.
[16] S.W. Lee, B.-S. Kim, S. Chen, y. Shao-Horn, P.T. Hammond, J. Am. Chem. Soc. 131 (2009) 671.
[17] L. Besra, M. Liu, Prog. Mater. Sci. 52 (2007) 1.
[18] K.S. Novoselov, Science 306 (2004) 666.
[19] Z.-S. Wu, W. Ren, L. Gao, J. Zhao, Z. Chen, B. Liu, B. Tang, B. Yu, C. Jiang, H.-M. Cheng, ACS Nano 3 (2009) 411.
[20] D. Li, M.B. Müller, S. Gilje, R.B. Kaner, G.G. Wallace, Nat. Nanotechnol. 3 (2008) 101.
[21] H. Chen, M.B. Müller, K.J. Gilmore, G.G. Wallace, D. Li, Adv. Mater. 20 (2008) 3557.

[22] D. Wang, D. Choi, J. Li, Z. Yang, Z. Nie, R. Kou, D. Hu, C. Wang, L.V. Saraf, J. Zhang, I.A. Aksay, J. Liu, ACS Nano 3 (2009) 907.
[23] J. Du, X. Lai, N. Yang, J. Zhai, D. Kisailus, F. Su, D. Wang, L. Jiang, ACS Nano 5 (2011) 590.
[24] A.L.M. Reddy, A. Srivastava, S.R. Gowda, H. Gullapalli, M. Dubey, P.M. Ajayan, ACS Nano 4 (2010) 6337.
[25] D. Boukhvalov, M. Katsnelson, A. Lichtenstein, Phys. Rev. B: Condens. Matter Mater. Phys. 77 (2008) 035427.
[26] K. Xue, Z. Xu, Appl. Phys. Lett. 96 (2010) 063103.
[27] S.R.C. Vivekcha, C.S. Rout, K.S. Subrahmanyam, A. Govindaraj, C.N.R. Rao, J. Chem. Sci. 120 (2008) 9.
[28] C. Liu, Z. Yu, D. Neff, A. Zhamu, B.Z. Jang, Nano Lett. 10 (2010) 4863.
[29] C. Du, N. Pan, J. Power Sources 160 (2006) 1487.
[30] I. Bispo-Fonseca, J. Aggar, C. Sarrazin, P. Simon, J.F. Fauvarque, J. Power Sources 79 (1999) 238.
[31] L. Cooper, H. Amano, M. Hiraide, S. Houkyou, I.Y. Jang, Y.J. Kim, H. Muramatsu, J.H. Kim, T. Hayashi, Y.A. Kim, M. Endo, M.S. Dresselhaus, Appl. Phys. Lett. 95 (2009) 233104.
[32] C. Shan, H. Yang, D. Han, Q. Zhang, A. Ivaska, L. Niu, Langmuir 25 (2009) 12030.
[33] Y. Si, E.T. Samulski, Nano Lett. 8 (2008) 1679.
[34] S. Niyogi, E. Bekyarova, M.E. Itkis, H. Zhang, K. Shepperd, J. Hicks, M. Sprinkle, C. Berger, C.N. Lau, W.A. deHeer, E.H. Conrad, R.C. Haddon, Nano Lett. 10 (2010) 4061.
[35] M. Chhowalla, A.C. Ferrari, J. Robertson, G.A.J. Amaratunga, Appl. Phys. Lett. 76 (2000) 1419.
[36] M.S. Dresselhaus, G. Dresselhaus, R. Saito, A. Jorio, Phys. Rep. 409 (2005) 47.
[37] A.C. Ferrari, B. Kleinsorge, N.A. Morrison, A. Hart, J. Appl. Phys. 85 (1999) 7191.
[38] A.C. Ferrari, J. Robertson, Phys. Rev. B 61 (2000) 14095.
[39] V.A. Coleman, R. Knut, O. Karis, H. Grennberg, U. Jansson, R. Quinlan, B.C. Holloway, B. Sanyal, O. Eriksson, J. Phys. D 41 (2008) 062001.
[40] Y. Wang, Z. Shi, Y. Huang, Y. Ma, C. Wang, M. Chen, Y. Chen, J. Phys. Chem. C 113 (2009) 13103.
[41] B.E. Conway, Electrochemical Supercapacitor: Scientific Fundamentals and Technological Application, Kluwer Academic/Plenum Publishers, New York, 1999.
[42] C. Du, J. Yeh, N. Pan, Nanotechnology 16 (2005) 350.